Journal Pre-proof

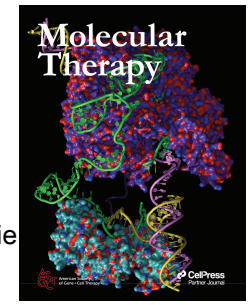

GITRL enhances cytotoxicity and persistence of CAR-T cells in cancer therapy

Binghe Tan, Chuntian Tu, Hao Xiong, Yongqian Xu, Xiujuan Shi, Xiaolin Zhang, Ruijie Yang, Na Zhang, Boxu Lin, Mingyao Liu, Juliang Qin, Bing Du

PII: S1525-0016(25)00040-1

DOI: https://doi.org/10.1016/j.ymthe.2025.01.036

Reference: YMTHE 6750

To appear in: *Molecular Therapy*

Received Date: 23 July 2024

Accepted Date: 22 January 2025

Please cite this article as: Tan B, Tu C, Xiong H, Xu Y, Shi X, Zhang X, Yang R, Zhang N, Lin B, Liu M, Qin J, Du B, GITRL enhances cytotoxicity and persistence of CAR-T cells in cancer therapy, *Molecular Therapy* (2025), doi: https://doi.org/10.1016/j.ymthe.2025.01.036.

This is a PDF file of an article that has undergone enhancements after acceptance, such as the addition of a cover page and metadata, and formatting for readability, but it is not yet the definitive version of record. This version will undergo additional copyediting, typesetting and review before it is published in its final form, but we are providing this version to give early visibility of the article. Please note that, during the production process, errors may be discovered which could affect the content, and all legal disclaimers that apply to the journal pertain.

© 2025 The American Society of Gene and Cell Therapy. Published by Elsevier Inc. All rights are reserved, including those for text and data mining, AI training, and similar technologies.

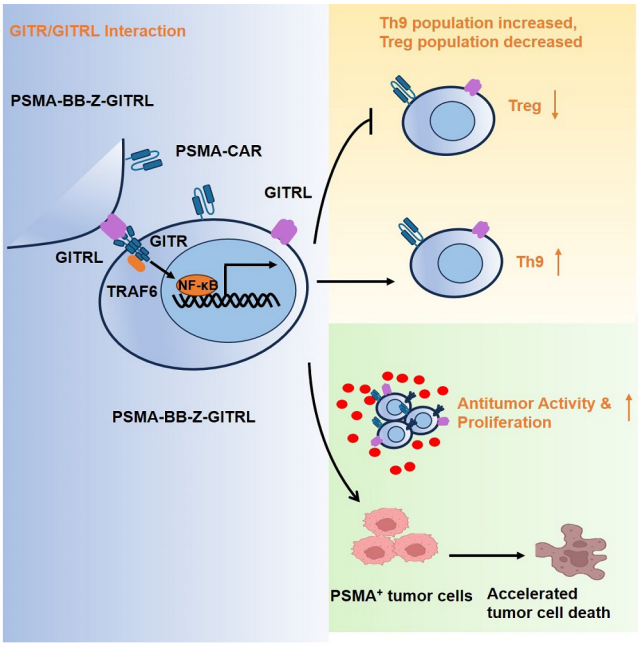

Journal Pre-proof

GITRL enhances cytotoxicity and persistence of CAR-T cells in cancer therapy

Binghe Tan[1,2#], Chuntian Tu[1,#], Hao Xiong[1,#], Yongqian Xu[1], Xiujuan Shi[1], Xiaolin Zhang[1], Ruijie Yang[1], , Na Zhang[1,2], Boxu Lin[1], Mingyao Liu[1], Juliang Qin[1,*], Bing Du[1,*]

1. Shanghai Frontiers Science Center of Genome Editing and Cell Therapy, Shanghai Key Laboratory of Regulatory Biology and School of Life Sciences, East China Normal University, Shanghai, China, 200241.

2. BRL Medicine Inc. Shanghai, China, 201109.

[#] These authors contribute equally to this work.

Short title: GITRL enhances CAR-T cell's cytotoxicity and persistence

Corresponding Authors: Bing Du, Ph.D., Institute of Biomedical Sciences and School of Life Sciences, East China Normal University, 500 Dongchuan Road, Shanghai 200241, China; Tel: +86-21-24206964; Fax: +86-21-54344922; E-mail: bdu@bio.ecnu.edu.cn; Juliang Qin, Email: jlqin@bio.ecnu.edu.cn.

Journal Pre-proof

ABSTRACT

CAR T-cell therapy has achieved remarkable clinical success in treating hematological malignancies. However, its clinical efficacy in solid tumors is less satisfactory, partially due to poor *in vivo* expansion and limited persistence of CAR-T cells. Here, we demonstrated that the overexpression of glucocorticoid-induced tumor necrosis factor receptor-related protein ligand (GITRL) enhances the anti-tumor activity of CAR-T cells. Compared to PSMA-BB-Z CAR-T, PSMA-BB-Z-GITRL CAR-T cells have much more IFN-γ, TNF-α, and IL-9 secretion, a higher proportion of central memory T (T_{CM}) cells and Th9 cells, less expression of exhaustion markers, and robust proliferation capacity. Consequently, PSMA-BB-Z-GITRL CAR-T cells exhibited more potent anti-tumor activity against established solid tumors *in vivo* than PSMA-BB-Z CAR-T cells. The results of *in vivo* persistence experiment also indicated that PSMA-BB-Z-GITRL CAR-T cells exhibited much more retention in mouse blood, spleen, and tumor tissue than PSMA-BB-Z CAR-T cells 15 days after CAR-T cell therapy. In addition, PSMA-BB-Z-GITRL CAR-T cells produce higher levels of IFN-γ, TNF-α and IL-9 in mouse blood, exhibiting a higher proportion of T_{CM} cells and a lower proportion of Treg cells compared to PSMA-BB-Z CAR-T cells. Our results demonstrate that the overexpression of GITRL has important implications for improving CAR-T cell-based human solid tumor immunotherapy.

Journal Pre-proof

INTRODUCTION

As an emerging adoptive T cell therapy, CAR-T cell therapy has made remarkable achievements in treating hematological malignancies[1-5]. However, the efficacy of CAR-T cells in solid tumors remains far from satisfactory, mainly because of limited tumor trafficking, infiltration and immunosuppressive tumor microenvironment[6-8]. Different approaches have been used to overcome the immunosuppressive tumor microenvironment (TME), the including remodeling of immunosuppressive cells and developing armored CAR-T cells that secrete immunostimulatory cytokines and co-stimulatory molecules[9]. However, the outcomes of CAR-T therapy in solid tumors have not been enhanced[10].

Although more than 11 types of CAR-T cells have been approved for commercial applications, all are generated from the second-generation CARs (Chimeric Antigen Receptor, CAR) with co-stimulatory domains derived from CD28 or 4-1BB[11]. T-cell activation is a complicated and carefully regulated process involving in many additional signals from co-stimulatory molecules and cytokines. Although preclinical data have not demonstrated consistent superior anticancer activity with CARs containing either a CD28 or a 4-1BB co-stimulatory domain, the persistence of T cells with CARs containing a 4-1BB domain seems to be better in some mouse models[12]. The longer persistence of 4-1BB CAR-T cells has been correlated with slower or less complete tumor clearance than CD28 CAR-T cells[13]. Recent studies showed that introducing a second co-stimulatory molecule, such as CD28, ICOS, or NKG2D into CAR-T cells with 4-1BB as the primary

co-stimulatory molecule yielded better therapeutic effects compared to CAR-T cells with 4-1BB alone[14,15]. Thus, CAR-T cells may benefit from discovering new co-stimulatory pathways and exploiting known accessory molecules.

The glucocorticoid-induced TNFR-related receptor (GITR) is a type I transmembrane protein with a cysteine-rich extracellular domain. Although the cytoplasmic domain of GITR shares homology with TNFR family members 4-1BB and CD28, GITR uses TRAF2 and TRAF5 for the NF-κB-dependent upregulation of Bcl-xL[16-18]. GITR signaling enhances the differentiation of $CD4^+$ T helper (Th9) cells to promote the production of IL-9 in a TNFR-associated factor 6 (TRAF6) and NF-κB-dependent manner, enhancing CTL-mediated anti-tumor immune responses[19]. GITR is not only highly expressed on activated Teff cells but also highly expressed on Treg cells. Therefore, the agonistic antibody (αGITR) alleviates Treg cell-mediated suppression of the anti-tumor immune response by facilitating the differentiation of Treg cells into Teff cells[19-21]. GITR agonism using the anti-GITR antibody TRX518 reduced circulating and intertumoral Treg cells in patients with advanced cancer (NCT01239134) [22]. However, monotherapy appears ineffective, whereas responses have been reported when combined with PD-1 blockade.

Increasing evidence indicates that IL-9-producing T cells may have potent abilities to eradicate advanced tumors[23]. The activation of CAR-T cells by GITR was more significant than by 4-1BB or CD28, suggesting the superiority of GITR signaling in T cell-mediated anti-tumor immunity. Therefore, we co-expressed the GITR ligand (GITRL) on 4-1BB-based CAR-T cells to achieve self-sustaining activation of GITR on CAR-T cells. Our data

showed that the proliferation, cytotoxicity, and granzyme expression were significantly increased in PSMA-BB-Z-GITRL CAR-T cells. The *in vivo* anti-tumor activity and persistence of PSMA-BB-Z cells were enhanced considerably by GITRL, suggesting that GITRL-expressing CAR-T cells have great potential for treating solid tumors.

RESULTS

GITRL influenced the T cell differentiation and phenotypes

To determine the role of GITR signaling in regulating T cell differentiation, $CD3^+$ T cells were sorted from healthy donor-derived PBMC and stimulated with anti-CD3/CD28 in the presence of IL-2. These cells were treated with the GITR ligand fusion protein (GITR-L) for 3 days. The proportion of T_{CM} cells was significantly increased by GITR-L (Figure 1A), whereas the percentage of Treg cells was reduced considerably by GITR-L (Figure 1B), consistent with previous reports[19,24]. Adding GITR-L increased the expression level of IL-9 mRNA in T cells, and the protein expression level of IL-9 in T cells was GITR-L (Figures 1C and 1D). The ratio of CD4 and CD8 cells was slightly altered by GITR-L (Figure 1E). Given that GITR-L can decrease the ratio of Treg cells and increase the ratio of T_{CM} cells and Th9 cells in T cells, we co-expressed GITRL with CAR-T cells to facilitate the potential of CAR-T cells to eliminate cancer cells. We constructed second-generation 4-1BB based CAR-T cells targeting CD19 (CD19-BB-Z and CD19-BB-Z-GITRL) or PSMA (PSMA-BB-Z and PSMA-BB-Z-GITRL) with or without GITRL overexpression (Figure 1F and Figures S1A and S1B). After lentiviral infection, CAR-T cell positivity was > 65% (Figure 1G and

Figure S1C) and was maintained for a long time (Figure 1H and Figure S1D). Additionally, GITRL expression was highly increased in both PSMA-BB-Z-GITRL and CD19-BB-Z-GITRL cells (Figure 1I and Figure S1E). Furthermore, the overexpression of GITRL did not affect the proportion of $CD4^+$ and $CD8^+$ T cells in response to tumor antigen stimulation (Figure 1J). In summary, GITR-L increased the differentiation of Th9 and T_{CM} cells but decreased that of Treg cells, which has excellent potential to enhance the anti-tumor immunity of CAR-T cells.

GITRL enhances the cytotoxicity and the activation of CAR-T cells *in vitro*

To explore the function of GITRL in CAR-T cells, CAR-T cells with or without GITRL were co-cultured with $PSMA^+$ PC3 cells at different effector-to-target ratios. Although cancer cells could be eliminated significantly by all CAR-T cells, the cytotoxicity was higher in GITRL co-expressed CAR-T cells (Figure 2A and Figure S2A). Most importantly, the GITRL expressed CAR-T cells were demonstrated to have the advantage of avoiding cancer cells-mediated immunosuppression (Figure 2B) and sustaining cytotoxicity against tumor cells (Figure 2C). Similar results were obtained for CD19-BB-Z and CD19-BB-Z-GITRL CAR-T cells (Figure S2B). In addition, T cell activation markers, such as CD25 and CD69, were dramatically increased in PSMA-BB-Z-GITRL CAR-T cells (Figures 2D and 2E). The expression of CD107a, TNF-α and IFN-γ, all effector molecules of T cell-mediated cytotoxicity, was also enhanced in PSMA-BB-Z-GITRL CAR-T cells (Figures 2F–H). Meanwhile, the concentration of TNF-α and IFN-γ in the cultured PSMA-BB-Z-GITRL

CAR-T cells' cultured supernatant was increased (Figures 2I and 2J). Similar data were also detected in the co-cultured supernatant of CD19-BB-Z-GITRL CAR-T cells (Figures S2C and S2D). Our findings indicate that after co-culture with $PC3^+$ PSMA cells, the cytotoxicity and cytokine release levels of PSMA-BB-Z-GITRL were significantly enhanced compared to those of PSMA-BB-Z.

GITRL promotes proliferation and reduces exhaustion of CAR-T cells

The proliferation of CAR-T cells after antigen stimulation is one of the most important indicators of long-term CAR-T cell killing. After co-culturing CAR-T cells with $PC3^+$ PSMA cells, the rapid and increased proliferation of PSMA-BB-Z-GITRL CAR-T cells was observed (Figure 3A). The expression of most cell cycle progression- and proliferation-associated marker genes, such as *Cdks*, *Aurkb,* and *Mapks*, was enhanced in PSMA-BB-Z-GITRL CAR-T cells (Figure 3B). More S/G2 phase cells were observed in PSMA-BB-Z-GITRL T cells (Figure 3C). Apoptotic cells were restricted to PSMA-BB-Z-GITRL CAR-T cells (Figure 3D). The proportion of Treg cells was significantly reduced in PSMA-BB-Z-GITRL CAR-T cells after with $PC3^+$ PSMA cells for 5 days (Figure 3E). Accordingly, the distribution of immune checkpoints, including PD-1 and TIM-3, was restricted in PSMA-BB-Z-GITRL CAR-T cells after treatment with $PC3^+$ PSMA (Figure 3F). T_{CM} cells have long-term antigen-specific memory, rapid activation capabilities, the ability to expand and migrate quickly, and persist in the circulation and lymph nodes for a long time[25,26]. Consistent with the GITRL-treated T cells (Figure 1A), the proportion of $CCR7^+$ $CD45RO^+$

T_{CM} cells was significantly enhanced in PSMA-BB-Z-GITRL CAR-T cells after co-culturing with $PC3^{+}$ PSMA cells (Figure 3G). Taken together, co-expression of GITRL in CAR-T cells not only promotes the proliferation of CAR-T cells and the formation of T_{CM} cells but also reduces CAR-T cell exhaustion and apoptosis, showing the considerable potential of GITRL overexpressed CAR-T cells in fighting solid tumors.

The MYC and NF-κB associated signaling were increased in PSMA-BB-Z-GITRL CAR-T cells

To investigate the mechanism by which GITRL affects CAR-T cells, we co-cultured PSMA-BB-Z and PSMA-BB-Z-GITRL CAR-T cells with $PSMA^{+}$ PC3 cells for 12 hours and collected three CAR-T cell samples from each group for RNA sequencing. The GO enrichment analysis of these differential genes showed that the pathways of "Genes regulated by NF-κB in response to TNF," "Genes defining inflammatory response," "Genes up-regulated by STAT5 in response to IL2 stimulation," and "Genes up-regulated in response to IFNG" were all highly enriched in PSMA-BB-Z-GITRL CAR-T cells (Figure 4A). These pathways regulate T-cell inflammatory responses, activation and proliferation, and cytokine production. We performed a qPCR to confirm that GITRL influenced the signature genes. The expression of *Nr4a1* and *Fos*, which positively regulated the NF-κB pathway, was significantly upregulated in the PSMA-BB-Z-GITRL group (Figure 4B). In contrast, the expression of *Tnfaip2*, *Klf4*, and *Abca1*, which negatively regulated the NF-κB pathway, was significantly downregulated. Genes related to cytotoxicity, including *Gzma*, *Gzmb*,

167 *Gzmm*, *Ifn-γ*, and *Tnf-α*, were significantly upregulated (Figure 4B). Genes associated with
168 proliferation and cell cycle, including *Cct4*, *Cct2*, *Cct7*, *Nme1*, and *Ggr1*, were significantly
169 upregulated (Figure 4B). Genes associated with T cell differentiation, including *Il4*, *Il6*, and
170 *Il9*, were also significantly upregulated (Figure 4B). Gene Set Enrichment Analysis (GSEA)
171 showed that genes associated with MYC TARGETS V1, MYC TARGETS V2, G2M
172 CHECKPOINT, PI3K AKT MTOR SIGNALING, E2F TRANSCRIPTION FACTORS and
173 MTORC1 COMPLEX were significantly enriched in PSMA-BB-Z-GITRL CAR-T cells
174 (Figures 4C–H). These data suggest that co-expression of GITRL enhances T cell
175 proliferation, differentiation, and immune activity in MYC- and NF-κB-associated signaling
176 pathways.
177 PSMA-BB-Z-GITRL CAR-T cells exhibited significant proliferation potential, with
178 upregulation of the MYC-related genes *Cdk2* and *Cdk4*, which may increase the risk of
179 uncontrolled proliferation and carcinogenesis. Consequently, we further assessed the
180 proliferation curves of PSMA-BB-Z-GITRL CAR-T cells within 24 days post-stimulation
181 with PC3- PSMA and changes in *Cdk2* and *Cdk4* transcription levels within 14 days. The
182 results indicated a decline in the PSMA-BB-Z-GITRL CAR T-cell population after 21 days,
183 suggesting no uncontrolled proliferation (Figure S3A). Furthermore, CDK2 and CDK4
184 transcript levels showed no significant differences on days 9 post-stimulation (Figure S3B).
185
186 **GITRL facilitates Th9 cell differentiation through TRAF6-NF-κB signaling pathway**
187 In addition to Th1 cells, Th9 cells also trigger potent anti-tumor activity in a mouse model

of melanoma[27]. The number of Th9 cells is negatively associated with metastatic melanoma lesions[28-31]. These findings indicate that enhancing the Th9 response is a promising immunotherapeutic strategy for human cancer treatment. Our findings showed that PSMA-BB-Z CAR-T cells that overexpressing GITRL exhibited a significantly higher secretion of IL-9 (Figure 5A). Furthermore, the proportion of Th9 cells increased nearly three-fold compared to that of PSMA-BB-Z CAR-T cells (from approximately 2.5% to 8.6%) (Figure 5B), consistent with the enhanced production of IL-9. To further elucidate the molecular mechanisms directing Th9 differentiation by GITRL, we analyzed multiple transcription factors crucial for Th9 cell differentiation. Kinetic analyses showed that *Pu.1*, *Gata3*, and *Irf4* transcription levels remained unchanged or were slightly upregulated in PSMA-BB-Z-GITRL CAR-T cells (Figure 5C). Although GITR interacted with *Traf2*, *Traf5*, and *Traf6* in T cells, only *Traf6* was significantly upregulated in PSMA-BB-Z-GITRL CAR-T cells (Figure 5C). The levels of p-P65 in PSMA-BB-Z-GITRL CAR-T cells were considerably higher than in PSMA-BB-Z CAR-T cells at multiple time points (Figure 5D). To further validate that overexpression of GITRL enhanced the cytotoxic efficacy of CAR-T cells against tumor cells via the NF-κB pathway and facilitates the differentiation of CAR-T cells into Th9 cells, we evaluated the IL-9 secretion and cytotoxic capabilities of PSMA-BB-Z and PSMA-BB-Z-GITRL CAR-T cells under conditions both with and without the NF-κB inhibitor (BAY 11-7082). Following treatment with BAY 11-7082, the results indicated that PSMA-BB-Z-GITRL and PSMA-BB-Z CAR-T cells demonstrated comparable levels of IL-9 secretion and cytotoxicity against tumor cells (Figures 5E and 5F), strongly

209 suggesting that GITRL-induced Th9 differentiation occurs mainly via the TRAF6–NF-κB
210 signaling pathway.
211
212 **GITRL enhances the anti-tumor efficacy of CAR-T cells in mouse model**
213 To evaluate the therapeutic efficacy of GITRL *in vivo*, subcutaneous xenografts were
214 established by injecting stable luciferase-transfected $PC3^{+}$ PSMA cells (PC3-PSMA-LUC)
215 into NSG mice. After 10 days, the mice were randomly divided into three groups of 6 mice
216 per group and subjected to intravenous injections of Control T cells, PSMA-BB-Z CAR-T
217 cells, or PSMA-BB-Z-GITRL CAR-T cells (Figure 6A). Bioluminescence imaging showed
218 sustained tumor regression by PSMA-BB-Z and PSMA-BB-Z-GITRL CAR-T cells
219 compared with Control T cells; it was demonstrated that mice treated with PSMA-BB-Z-
220 GITRL CAR-T cells exhibited significantly more tumor regression than those treated with
221 PSMA-BB-Z CAR-T cells (Figures 6B–D). The PSMA-BB-Z-GITRL CAR-T cell treatment
222 group showed a considerably longer survival time for mice than the PSMA-BB-Z CAR-T
223 cell treatment group (Figure 6E). During treatment, we monitored the $CD3^{+}CAR^{+}$ T cell
224 counts in the peripheral blood of mice across each treatment group on days 7, 14, and 21
225 following the initiation of treatment. The experimental findings demonstrated that the
226 retention of PSMA-BB-Z-GITRL CAR T cells in the bloodstream was significantly greater
227 than that of PSMA-BB-Z CAR T cells at all evaluated time points (Figure 6F). In conclusion,
228 the data indicate that the anti-tumor efficacy of PSMA-BB-Z-GITRL CAR-T cells is
229 significantly enhanced compared to traditional CAR-T cells, suggesting substantial

potential for treating metastatic castrate-resistant prostate cancer.

GITRL enhanced the *in vivo* persistence of CAR-T cell anti-tumor activity

PSMA-BB-Z-GITRL CAR-T cells exhibited increased proportions of T_{CM} and Th9 cells (Figures 3G and 5B) and enhanced antitumor activity *in vitro* (Figures 2G and 2H). This encouraged us to assess further its potency in xenograft tumor models (Figure 7A). After a 15-day treatment period, the serum concentrations of TNF-α, IFN-γ, and IL-9 in mice administered PSMA-BB-Z-GITRL CAR-T cells were significantly elevated compared to those in mice treated with PSMA-BB-Z CAR-T cells (Figure 7B). The proportion of T_{CM} cells in PSMA-BB-Z-GITRL CAR-T cells in the peripheral blood of mice was significantly increased, whereas the proportion of Treg cells was significantly decreased (Figure 7C). The total count of $CD3^+$ T cells and the number of $CD3^+$ T cells infiltrating the tumor within the spleen in the PSMA-BB-Z-GITRL CAR-T cell treatment group were increased significantly (Figures 7D and 7E). No significant pathological changes were observed by H&E (Hematoxylin and Eosin, H&E) staining in the tissues of either group of mice, indicating that treatment with PSMA-BB-Z or PSMA-BB-Z-GITRL CAR-T cells did not cause any side effects (Figure 7F). Given that PSMA-BB-Z-GITRL CAR-T cells exhibited accelerated tumor clearance. They enhanced the retention of $CD3^+$ T cells in xenograft tumor models; we constructed a rechallenge model to evaluate the efficacy of PSMA-BB-Z-GITRL CAR-T cells in eliminating the subsequent rounds of PC3-PSMA cells that had been engrafted with tumors (Figure 7G). Rechallenge assay revealed that the adoptive

transfer of PSMA-BB-Z-GITRL CAR-T cells exhibited accelerated kinetics in tumor clearance, leading to complete tumor regression by day 28. Even after a second rechallenge with tumor cells on day 28, the PSMA-BB-Z-GITRL CAR-T cells maintained their capacity to inhibit tumor formation (Figure 7H). In conclusion, overexpression of GITRL significantly increased the infiltration of CAR-T cells into murine tumor tissues and improved their retention in the spleen. It endowed PSMA-BB-Z-GITRL CAR-T cells with the ability to eliminate subsequent rounds of tumor cells. These findings suggest that this strategy represents a promising therapeutic approach for managing metastatic and advanced prostate cancers.

DISCUSSION

The clinical response to B cell malignancies is correlated with CAR-T cells' *in vivo* expansion and persistence. However, it has been found during the treatment of solid tumors that CAR-T cells do not have robust proliferation capacity and persistence, and there is a lack of strong efficacy demonstrated in trials reported to date[14]. Here, we investigated whether CAR-T cells' expansion capability, persistence, and efficacy could be improved by adding high-quality co-stimulatory domains. GITR is a member of the TNF superfamily of proteins that regulates immune responses, along with other members such as 4-1BB, OX-40, CD27, etc. GITR can be activated by its ligand (GITRL), which costimulates T cells[32]. Notably, the downstream signaling pathways of GITR and 4-1BB, which work together to exert their functions, are not identical and have complementary

effects. Our results also demonstrated that GITRL overexpression significantly enhanced the cytotoxicity of PSMA-BB-Z CAR-T cells against tumor cells. We also found that GITRL overexpression enhanced the sustained cytotoxicity of PSMA-BB-Z CAR-T cell-mediated killing of tumor cells, which may be attributed to PSMA-BB-Z-GITRL CAR-T cells having a higher proportion of T_{CM}, lower expression of exhaustion markers, and a faster expansion rate under tumor stimulation. We analyzed the RNA-seq data to dissect the transcriptional features of PSMA-BB-Z-GITRL CAR-T cells. The results indicate that compared to PSMA-BB-Z CAR-T cells, the transcript levels of genes associated with cell proliferation and activation, including *Cdks*, *Mapks*, *BATF*, *Pu.1*, and *Fos*, and genes related to cytotoxicity such as *Gzma*, *Gzmb*, *Gzmm*, *Ifn-γ*, and *Tnf-α*, increase significantly in PSMA-BB-Z-GITRL CAR-T cells. Changes in the transcript levels of these genes revealed the underlying mechanisms by which GITRL overexpression promotes the expansion, activation, and cytotoxicity of PSMA-BB-Z CAR-T cells.

Treg cells are one of the main obstacles in cancer immunotherapy, and the tumor microenvironment can expand the population of Treg cells[33]. Both GITR agonists and GITR-L, the ligand for GITR, can effectively inhibit the generation of regulatory T cells both *in vivo* and *in vitro*[19,21]. Our results also showed that overexpression of GITRL in PSMA-BB-Z CAR-T cells led to a significant decrease in the frequency of $CD4^+Foxp3^+$ cells both *in vivo* and *in vitro* under tumor stimulation, resulting in a shift in the balance of Treg cells towards effector T cells and T_{CM}. GITRL is constitutively expressed in APCs in the tumor microenvironment[34]. Studies have found that the physiological interaction between GITR

and GITRL may help induce Th9 cells, suggesting that GITR may play a tumor-suppressive role by inducing a Th9 cell response against malignant tumors. However, due to the weak physiological GITR signal, which cannot induce sufficient amounts of IL-9, we overexpressed GITRL in PSMA-BB-Z CAR-T cells via lentiviral infection to enhance the GITR signal and induce an optimal anti-tumor immune response. Consistent with previous reports, we found in both *in vivo* and *in vitro* experiments that PSMA-BB-Z-GITRL CAR-T cells induced higher levels of IL-9 compared to PSMA-BB-Z CAR-T cells. The induction of a higher number of Th9 cells by GITR-GITRL interactions may be one of the reasons why PSMA-BB-Z-GITRL CAR-T cells exhibit fewer exhausted, fully cytolytic, and hyper-proliferative properties, as CAR-T cells constructed using Th9 cells have been reported to exhibit such characteristics[35].

To achieve optimal Th9 differentiation, the integration of multiple signals is required [36-39]. Previous studies have shown that GITR signaling promotes Th9 differentiation through two different mechanisms: (I) activation of the TRAF6-NF-κB pathway and (II) increased production of IL-4[19]. We analyzed the expression of genes related to these two different mechanisms. We found that the expression of *Traf6* and *Il-4* in PSMA-BB-Z-GITRL CAR-T cells was significantly upregulated, and the phosphorylation level of the P65 protein was also higher than that in PSMA-BB-Z CAR-T cells. Moreover, the experiment inhibiting the NF-κB pathway confirmed that the enhanced secretion of IL-9 and the anti-tumor efficacy of PSMA-BB-Z-GITRL CAR-T cells are contingent upon a more pronounced activation of

the NF-κB pathway. Therefore, we speculate that the synergistic effect of these two mechanisms promotes the differentiation of PSMA-BB-Z-GITRL CAR-T cells into Th9 cells via the NF-κB pathway *in vivo* and *in vitro*.

In summary, we designed and prepared enhanced CAR-T cells by co-expressing GITRL. *In vitro* and *in vivo* experiments showed that these novel CAR-T cells could enhance anti-tumor efficacy, have stronger proliferative ability, and delay CAR-T cell exhaustion, thus enhancing the sustainability of CAR-T cells to exert anti-tumor functions. Our study revealed the important role of activating GITR, a co-stimulatory molecule, in enhancing the anti-tumor function of CAR-T cells, providing a new perspective for treating solid tumors with CAR-T cells.

MATERIALS AND METHODS

Mice

This study utilized male NSG (NOD/SCID/IL-2RG) mice aged 6 to 8 weeks, which were procured from GemPharmatech. The NSG mice were maintained in a specific pathogen-free (SPF) facility at East China Normal University. Standardized feeding protocols were adhered to, and all equipment and materials employed in the study underwent sterilization via autoclaving at elevated temperatures and pressures to minimize any potential contamination. All animal experiments were conducted within the animal facility and received approval from the Ethics Committee of East China Normal University.

Cell lines and culture condition

Peripheral blood samples for CAR-T cell isolation were collected from healthy volunteers (minimum of three individuals) who provided informed consent. All blood samples were collected and handled according to the ethical and safety procedures approved by the Clinical Ethics Committee of the First Affiliated Hospital, College of Medicine, Zhejiang University. PBMCs were isolated using lymphocyte separation medium (TBD Science, LTS10770015). $CD3^+$ T cells were isolated from PBMCs using the CD3 MACS kit (Miltenyi) and activated using the T Cell TransActTM kit (Miltenyi). The PC3 was acquired from the American Type Culture Collection (ATCC) and maintained in RPMI 1640 medium (Gibco) with 10% fetal bovine serum (FBS) and 1% penicillin/streptomycin (P/S). The lentiviral-mediated overexpression of PSMA in PC3 cells was achieved, followed by selection with puromycin dihydrochloride (2-4 mg/mL; BBI Life Science, F118BA0026) for stable expression of PSMA and luciferase. The 293T cell line was procured from ATCC and cultured in DMEM medium (Gibco) with 10% FBS and 1% P/S at 37°C in a humidified atmosphere with 5% CO2.

Plasmid construction

To construct a second-generation CAR vector that facilitates the overexpression of GITRL, we synthesized the gene sequence corresponding to GITRL. The CAR was driven by the EF1α promoter, with its initial nucleotide sequence comprising the anti-human PSMA-scfv, CD8A, 4-1BB, and CD3ζ. The GITRL sequence was subsequently integrated at the

terminus of the initial nucleotide sequence through the use of the T2A peptide sequence. Ultimately, we successfully generated the PSMA-BB-Z plasmid, which contains solely the initial nucleotide sequence, as well as the PSMA-BB-Z-GITRL plasmid, which encompasses both nucleotide sequences.

Retrovirus and lentivirus preparation of CAR-T cells

The prepared CAR plasmid and lentivirus packaging plasmids (psPAX2 and pMD2.G) were co-transfected into 293T cells at a ratio of 5:5:3 to generate lentiviral particles. After transfection, cells were incubated at 37°C for 6-8 hours, then the medium was replaced and the cells were incubated for an additional 48 hours in fresh culture medium. The supernatant was collected, filtered through a 0.22 μm filter, and concentrated by centrifugation at 25,000 rpm for 2.5 hours at 4°C. The concentrated viral particles were dissolved and stored at -80°C.

Activated T cells, which had been cultured with CD3/CD28 magnetic beads for three days, were mixed with the viral particles at a ratio of 1:10, and centrifuged at 1000g for 2 hours at 32°C. After 3 days of infection, a small number of cells were collected to evaluate CAR expression using flow cytometry.

Flow cytometry

PBS containing 1% FBS was employed as the washing and staining buffer, whereas PBS with 4% FBS served as the blocking buffer. For extracellular marker staining, immune cells

or other dissociated single cells were washed twice and then incubated with the corresponding flow cytometry antibody for the desired marker at 4°C for 30 minutes. In the case of intracellular marker staining, immune cells or other dissociated single cells were initially stained with extracellular markers, Then, the cell membrane breaking and fixation kit (BD) were performed using at 4°C for 2 hours to allow for intracellular staining. For subsequent intracellular staining, the procedure is similar to that of extracellular staining. After staining, the cells were washed twice with PBS and analyzed on a FACSCalibur TM or LSR II flow cytometer (BD Biosciences). The acquired data were analyzed using FlowJo software (BD).

Quantitative RT–PCR and ELISA assay

The mRNA was extracted using an RNA extraction kit (Magen, R4801-02), following the manufacturer's instructions for extracting cellular RNA. Subsequently, the extracted mRNA was reverse transcribed into cDNA using a mRNA reverse transcription kit. The cDNA served as a template for subsequent real-time quantitative PCR analyses. The primer sequences employed for real-time fluorescent quantitative PCR analysis in this study are detailed in Table S2. The levels of IFN-γ, TNF-a and IL-9 were quantified using human IFN-γ (Invitrogen, 88-7316-88), human TNF-a (Invitrogen, 88-7346-88), and human IL-9 (R&D, DY361) ELISA kits, respectively, following the manufacturer’s instructions.

Western blot

For Western blot assays, CAR-T cells were co-cultured with PSMA$^+$ PC3 cells in a 1:1 ratio. At time intervals of 0, 15, 30, 60, and 120 minutes, the CAR-T cells were collected for subsequent analysis. The collected CAR-T cells were lysed using RAPI lysis buffer. Following lysis, the cell lysate was centrifuged at 12,000 rpm for 10 minutes at 4°C, and the supernatant was collected. The protein concentration was determined by the BCA assay. An equal amount of protein was loaded onto a 12.5% SDS-PAGE gel. Subsequently, the separated proteins were transferred onto a polyvinylidene difluoride filter (PVDF) membrane (Millipore, Bedford, MA, United States). The PVDF membrane was blocked with 5% non-fat milk in PBS buffer at room temperature for 2 hours, and incubated with primary antibody probe overnight at 4°C. The PVDF membrane was washed three times with TBST, and then incubated with the secondary antibody at room temperature for 1 hour.

Cytotoxicity assay

To ensure consistency, T cells from the same batch were used to adjust the CAR positivity rates of both CAR-T cells types. Subsequently, both were utilized as effector cells. The PC3$^+$ PSMA-LUC cells served as target cells. The effector cells and target cells were mixed at varying effector-to-target ratios (0.5:1, 1:1, 2:1) and subsequently incubated in a low-adhesion 96-well plate. After 16 hours, the cells were collected from the mixture, and 100 μL of the cell suspension was transferred to a new 96-well plate for fluorescent

measurement. For the cytotoxicity assay, 10 μL of luciferase substrate was added into each well, followed by fluorescent measurement.

In vivo killing assay and _in vivo_ retention assay

The subcutaneous xenograft model was established by injecting 2×10^6 PC3-PSMA-LUC cells subcutaneously into the right flank of 6-8-week-old male NSG (NOD-PrkdcscidIL2rgtm1/Bcgen, Beijing Biocytogen Co., Ltd.) mice. Subsequent experiments were performed 15 days post-establishment of the tumor model. When the average tumor size reached approximately 200 mm^3, the mice were divided equally into three treatment groups. For *in vivo* cytotoxicity assays, $1×10^6$ CAR-T cells were injected via tail vein. Bioluminescence imaging (BLI) was performed on days 3, 7, 10, and 15 using the Xenogen-IVIS imaging system (Caliper Life Sciences, Hopkinton, MA). Daily observations of the mice were conducted, and the number of surviving subjects was documented.

For the *in vivo* retention assays, the procedures for the subcutaneous xenograft model and CAR-T cell therapy were identical to those used in the cytotoxicity assays.15 days post-treatment, the hearts, lungs, kidneys, and livers of the mice were collected for H&E staining. Blood and spleen samples were also collected for flow cytometry analysis to evaluate T cell retention. All animal experiments were performed in accordance with protocols approved by the Institutional Animal Care and Use Committee of East China Normal University.

Statistical analysis

All data analyses and graphs were generated using Prism software (GraphPad) and presented as mean ± SD. Data comparisons were performed using one-way analysis of variance (ANOVA) in Primer 5.0 software, and survival curves were compared using the log-rank test. Each experiment was executed with a minimum of three biological replicates.

Keywords: CAR-T; GITRL; Central memory T; Th9; Solid tumor immunotherapy

ACKNOWLEDGMENTS

This work was supported by National Key R&D Program of China (2023YFC3402000 to B.D.); National Natural Science Foundation of China (32270960, 82430092 to B.D., 82173099 to J.Q.); Science and Technology Commission of Shanghai Municipality (23141901800, 23141903300); Shanghai Municipal Health Commission (2024CXJQ01); Program of Shanghai Academic/Technology Research Leader (23XD1430600); Shanghai Rising-Star Program (24QA2707300). We thank East China Normal University Multifunctional Platform for Innovation (011) and the Instruments Sharing Platform of School of Life Sciences at East China Normal University, for their technical assistance. We also acknowledge the valuable guidance and support provided by the Ethics Committee of East China Normal University (approval number m20190229) and the Ethics and Safety Procedures approved by the First Affiliated Hospital of Zhejiang University School of Medicine (IIT20210001C-R1 for Human Subjects) in conducting animal experiments in accordance with approved protocols and collecting and processing blood samples from volunteers.

DATA AVAILABILITY STATEMENT

The RNA-sequence datasets generated and analyzed in this study can be available from the corresponding authors upon request.

AUTHOR CONTRIBUTIONS

B.D., M.L. and B.T. designed the project, oversaw the experiments, analyzed the data, and wrote the manuscript. B.T., C.T., H.X., Y.X., X.S., X.Z., N.Z., and B.L. performed and analyzed the *in vitro* and *in vivo* experiments and data. J.Q. helped to oversaw the project, and contributed to data analysis and editing of the final version of the manuscript. All authors approved the final version of the manuscript.

DECLARATION OF INTERESTS

The authors declare no competing interests.

Journal Pre-proof

REFERENCES

1. Abreu, T.R., Fonseca, N.A., Gonalves, N., and Moreira, J.N. (2020). Current challenges and emerging opportunities of CAR-T cell therapies. J Control Release.
2. Fry, T.J., Shah, N.N., Orentas, R.J., Maryalice, S.S., Yuan, C.M., Sneha, R., Pamela, W., Staci, M., Cindy, D., and Bonnie, Y. (2017). CD22-targeted CAR T cells induce remission in B-ALL that is naive or resistant to CD19-targeted CAR immunotherapy. Nature Medicine *24*, nm.4441.
3. Grupp, S.A., Kalos, M., Barrett, D., Aplenc, R., Porter, D.L., Rheingold, S.R., Teachey, D.T., Chew, A., Hauck, B., and Wright, J.F. (2013). Chimeric antigen receptor-modified T cells for acute lymphoid leukemia. N Engl J Med.
4. Kalos, M., Levine, B.L., Porter, D.L., Katz, S., Grupp, S.A., Bagg, A., and June, C.H. (2011). T Cells with Chimeric Antigen Receptors Have Potent Antitumor Effects and Can Establish Memory in Patients with Advanced Leukemia. Science Translational Medicine *3*, 95ra73-95ra73.
5. Kochenderfer, J.N., Wilson, W.H., Janik, J.E., Dudley, M.E., Stetler-Stevenson, M., Feldman, S.A., Maric, I., Raffeld, M., Nathan, D.A., Lanier, B.J., et al. (2010). Eradication of B-lineage cells and regression of lymphoma in a patient treated with autologous T cells genetically engineered to recognize CD19. Blood *116*, 4099-4102. 10.1182/blood-2010-04-281931.
6. Beatty, G.L., and Moon, E.K. (2014). Chimeric antigen receptor T cells are vulnerable to immunosuppressive mechanisms present within the tumor microenvironment. Oncoimmunology *3*, e970027. 10.4161/21624011.2014.970027.
7. Beavis, P.A., Slaney, C.Y., Kershaw, M.H., Gyorki, D., Neeson, P.J., and Darcy, P.K. (2016). Reprogramming the tumor microenvironment to enhance adoptive cellular therapy. Seminars in immunology *28*, 64-72. 10.1016/j.smim.2015.11.003.
8. Joyce, J.A., and Fearon, D.T. (2015). T cell exclusion, immune privilege, and the tumor microenvironment. Science (New York, N.Y.) *348*, 74-80. 10.1126/science.aaa6204.
9. Chmielewski, M., and Abken, H. (2015). TRUCKs: the fourth generation of CARs. Expert opinion on biological therapy *15*, 1145-1154. 10.1517/14712598.2015.1046430.
10. Hartmann, J., Schüßler-Lenz, M., Bondanza, A., and Buchholz, C.J. (2017). Clinical development of CAR T cells-challenges and opportunities in translating innovative treatment concepts. EMBO molecular medicine *9*, 1183-1197. 10.15252/emmm.201607485.
11. Cappell, K.M., and Kochenderfer, J.N. (2021). A comparison of chimeric antigen receptors containing CD28 versus 4-1BB costimulatory domains. Nature reviews. Clinical oncology *18*, 715-727. 10.1038/s41571-021-00530-z.
12. Hamieh, M., Dobrin, A., Cabriolu, A., van der Stegen, S.J.C., Giavridis, T., Mansilla-Soto, J., Eyquem, J., Zhao, Z., Whitlock, B.M., Miele, M.M., et al. (2019). CAR T cell trogocytosis and cooperative killing regulate tumour antigen escape. Nature *568*, 112-116. 10.1038/s41586-019-1054-1.

13. Zhao, Z., Condomines, M., van der Stegen, S.J.C., Perna, F., Kloss, C.C., Gunset, G., Plotkin, J., and Sadelain, M. (2015). Structural Design of Engineered Costimulation Determines Tumor Rejection Kinetics and Persistence of CAR T Cells. Cancer cell *28*, 415-428. 10.1016/j.ccell.2015.09.004.
14. Guedan, S., Posey, A.D., Jr., Shaw, C., Wing, A., Da, T., Patel, P.R., McGettigan, S.E., Casado-Medrano, V., Kawalekar, O.U., Uribe-Herranz, M., et al. (2018). Enhancing CAR T cell persistence through ICOS and 4-1BB costimulation. JCI insight *3*. 10.1172/jci.insight.96976.
15. van der Stegen, S.J., Hamieh, M., and Sadelain, M. (2015). The pharmacology of second-generation chimeric antigen receptors. Nature reviews. Drug discovery *14*, 499-509. 10.1038/nrd4597.
16. Nocentini, G., Giunchi, L., Ronchetti, S., Krausz, L.T., Bartoli, A., Moraca, R., Migliorati, G., and Riccardi, C. (1997). A new member of the tumor necrosis factor/nerve growth factor receptor family inhibits T cell receptor-induced apoptosis. Proceedings of the National Academy of Sciences of the United States of America *94*, 6216-6221. 10.1073/pnas.94.12.6216.
17. Placke, T., Kopp, H.G., and Salih, H.R. (2010). Glucocorticoid-induced TNFR-related (GITR) protein and its ligand in antitumor immunity: functional role and therapeutic modulation. Clinical & developmental immunology *2010*, 239083. 10.1155/2010/239083.
18. Snell, L.M., Lin, G.H., McPherson, A.J., Moraes, T.J., and Watts, T.H. (2011). T-cell intrinsic effects of GITR and 4-1BB during viral infection and cancer immunotherapy. Immunological reviews *244*, 197-217. 10.1111/j.1600-065X.2011.01063.x.
19. Kim, I.K., Kim, B.S., Koh, C.H., Seok, J.W., Park, J.S., Shin, K.S., Bae, E.A., Lee, G.E., Jeon, H., Cho, J., et al. (2015). Glucocorticoid-induced tumor necrosis factor receptor-related protein co-stimulation facilitates tumor regression by inducing IL-9-producing helper T cells. Nat Med *21*, 1010-1017. 10.1038/nm.3922.
20. Amoozgar, Z., Kloepper, J., Ren, J., Tay, R.E., Kazer, S.W., Kiner, E., Krishnan, S., Posada, J.M., Ghosh, M., Mamessier, E., et al. (2021). Targeting Treg cells with GITR activation alleviates resistance to immunotherapy in murine glioblastomas. Nature communications *12*, 2582. 10.1038/s41467-021-22885-8.
21. Chan, S., Belmar, N., Ho, S., Rogers, B., Stickler, M., Graham, M., Lee, E., Tran, N., Zhang, D., Gupta, P., et al. (2022). An anti-PD-1-GITR-L bispecific agonist induces GITR clustering-mediated T cell activation for cancer immunotherapy. Nature cancer *3*, 337-354. 10.1038/s43018-022-00334-9.
22. Zappasodi, R., Sirard, C., Li, Y., Budhu, S., Abu-Akeel, M., Liu, C., Yang, X., Zhong, H., Newman, W., Qi, J., et al. (2019). Rational design of anti-GITR-based combination immunotherapy. Nat Med *25*, 759-766. 10.1038/s41591-019-0420-8.
23. Angkasekwinai, P., and Dong, C. (2021). IL-9-producing T cells: potential players in allergy and cancer. Nature reviews. Immunology *21*, 37-48. 10.1038/s41577-020-0396-0.
24. Xiao, X., Shi, X., Fan, Y., Zhang, X., Wu, M., Lan, P., Minze, L., Fu, Y.X., Ghobrial, R.M., Liu, W., et al. (2015). GITR subverts Foxp3(+) Tregs to boost Th9 immunity through

regulation of histone acetylation. Nature communications *6*, 8266. 10.1038/ncomms9266.

25. Fraietta, J.A., Lacey, S.F., Orlando, E.J., Pruteanu-Malinici, I., Gohil, M., Lundh, S., Boesteanu, A.C., Wang, Y., O'Connor, R.S., Hwang, W.T., et al. (2018). Determinants of response and resistance to CD19 chimeric antigen receptor (CAR) T cell therapy of chronic lymphocytic leukemia. Nat Med *24*, 563-571. 10.1038/s41591-018-0010-1.

26. Gattinoni, L., Klebanoff, C.A., Palmer, D.C., Wrzesinski, C., Kerstann, K., Yu, Z., Finkelstein, S.E., Theoret, M.R., Rosenberg, S.A., and Restifo, N.P. (2005). Acquisition of full effector function in vitro paradoxically impairs the in vivo antitumor efficacy of adoptively transferred CD8+ T cells. The Journal of clinical investigation *115*, 1616-1626. 10.1172/jci24480.

27. Lu, Y., Hong, S., Li, H., Park, J., Hong, B., Wang, L., Zheng, Y., Liu, Z., Xu, J., He, J., et al. (2012). Th9 cells promote antitumor immune responses in vivo. The Journal of clinical investigation *122*, 4160-4171. 10.1172/jci65459.

28. Nakatsukasa, H., Zhang, D., Maruyama, T., Chen, H., Cui, K., Ishikawa, M., Deng, L., Zanvit, P., Tu, E., Jin, W., et al. (2015). The DNA-binding inhibitor Id3 regulates IL-9 production in CD4(+) T cells. Nature immunology *16*, 1077-1084. 10.1038/ni.3252.

29. Nonomura, Y., Otsuka, A., Nakashima, C., Seidel, J.A., Kitoh, A., Dainichi, T., Nakajima, S., Sawada, Y., Matsushita, S., Aoki, M., et al. (2016). Peripheral blood Th9 cells are a possible pharmacodynamic biomarker of nivolumab treatment efficacy in metastatic melanoma patients. Oncoimmunology *5*, e1248327. 10.1080/2162402x.2016.1248327.

30. Purwar, R., Schlapbach, C., Xiao, S., Kang, H.S., Elyaman, W., Jiang, X., Jetten, A.M., Khoury, S.J., Fuhlbrigge, R.C., Kuchroo, V.K., et al. (2012). Robust tumor immunity to melanoma mediated by interleukin-9-producing T cells. Nat Med *18*, 1248-1253. 10.1038/nm.2856.

31. Rivera Vargas, T., Humblin, E., Végran, F., Ghiringhelli, F., and Apetoh, L. (2017). T(H)9 cells in anti-tumor immunity. Seminars in immunopathology *39*, 39-46. 10.1007/s00281-016-0599-4.

32. Krausz, L.T., Bianchini, R., Ronchetti, S., Fettucciari, K., Nocentini, G., and Riccardi, C. (2007). GITR-GITRL system, a novel player in shock and inflammation. TheScientificWorldJournal *7*, 533-566. 10.1100/tsw.2007.106.

33. Zou, W. (2006). Regulatory T cells, tumour immunity and immunotherapy. Nature reviews. Immunology *6*, 295-307. 10.1038/nri1806.

34. Stephens, G.L., McHugh, R.S., Whitters, M.J., Young, D.A., Luxenberg, D., Carreno, B.M., Collins, M., and Shevach, E.M. (2004). Engagement of glucocorticoid-induced TNFR family-related receptor on effector T cells by its ligand mediates resistance to suppression by CD4+CD25+ T cells. Journal of immunology (Baltimore, Md. : 1950) *173*, 5008-5020. 10.4049/jimmunol.173.8.5008.

35. Liu, L., Bi, E., Ma, X., Xiong, W., Qian, J., Ye, L., Su, P., Wang, Q., Xiao, L., Yang, M., et al. (2020). Enhanced CAR-T activity against established tumors by polarizing human T cells to secrete interleukin-9. Nature communications *11*, 5902. 10.1038/s41467-020-19672-2.

36. Angkasekwinai, P., Chang, S.H., Thapa, M., Watarai, H., and Dong, C. (2010). Regulation of IL-9 expression by IL-25 signaling. Nature immunology *11*, 250-256. 10.1038/ni.1846.

37. Elyaman, W., Bassil, R., Bradshaw, E.M., Orent, W., Lahoud, Y., Zhu, B., Radtke, F., Yagita, H., and Khoury, S.J. (2012). Notch receptors and Smad3 signaling cooperate in the induction of interleukin-9-producing T cells. Immunity *36*, 623-634. 10.1016/j.immuni.2012.01.020.

38. Perumal, N.B., and Kaplan, M.H. (2011). Regulating Il9 transcription in T helper cells. Trends in immunology *32*, 146-150. 10.1016/j.it.2011.01.006.

39. Yao, W., Zhang, Y., Jabeen, R., Nguyen, E.T., Wilkes, D.S., Tepper, R.S., Kaplan, M.H., and Zhou, B. (2013). Interleukin-9 is required for allergic airway inflammation mediated by the cytokine TSLP. Immunity *38*, 360-372. 10.1016/j.immuni.2013.01.007.

Journal Pre-proof

List of Figure Captions

Figure legends

Figure 1. The differentiation and phenotypes of T cells were modulated by GITR-L.

(A and B) Flow cytometric analysis was conducted to determine the proportions of T_{CM} ($CD45RO^+CCR7^+$) and Treg ($CD4^+CD25^+FOXP3^+$) in T cells. T cells were stimulated with human IgG protein (1 nM) antibody or human GITR-L protein (1 nM) for 3 days. (C) mRNA fold change of *Il-9* in T cells stimulated with human IgG protein (1 nM) antibody or human GITR-L protein (1 nM) for 24 hours. (D) The concentration of IL-9 in the supernatant of T cell cultures stimulated with a gradient of GITR-L protein concentrations for 2 day was measured by ELISA. (E) The $CD4^+/CD8^+$ T cell ratio of T cells after stimulation with GITR-L protein for 2 day was measured by flow cytometry. (F) Schematic representation of PSMA-targeted constructs with 4-1BB co-stimulatory domain, a CD3ζ domain, and a GITRL. (G) Flow cytometry analysis of the transduction efficiencies. (H) The expression levels of CAR at different time points were measured using flow cytometry. (I) The expression intensity of GITRL on CAR-T cells was measured by means of Flow cytometry. (J) Three days post-$PSMA^+$ PC3 cells stimulation, the proportion of $CD4^+/CD8^+$ T cells was determined by flow cytometry. All data with error bars represent the mean ± SEM of triplicate values resulting from 3 independent experiments performed under similar conditions. $^{NS}P>0.05$, $*P<0.05$, $**P<0.01$, $***P<0.001$. Student's t test.

Figure 2. GITRL enhanced the cytotoxicity and the activation of CAR-T cells *in vitro*.

(A) The cytotoxicity of Control T, PSMA-BB-Z, and PSMA-BB-Z-GITRL against $PSMA^+$ PC3 cells was evaluated at different effector/target (E:T) ratios for 16 hours. (B) Overexpression of GITRL enhances the tolerance of CAR-T cells to tumor culture supernatant. After stimulating CAR-T cells with medium containing 20% PC3-PSMA cell culture supernatant for 24 hours, the cytotoxicity of PSMA-BB-Z, and PSMA-BB-Z-GITRL CAR-T cells against PSMA+ PC3 cells was evaluated. (C) CAR-T cells were serially stimulated with $PSMA^+$ PC3 cells for three rounds at 16-hour intervals, the cytotoxicity of PSMA-BB-Z and PSMA-BB-Z-GITRL CAR-T cells against $PSMA^+$ PC3 cells was

evaluated 16 hours after each round of PSMA$^+$ PC3 cell addition. PSMA-BB-Z and PSMA-BB-Z-GITRL CAR-T cells were co-incubated with PSMA$^+$ PC3 cells at a 1:1 ratio for 24 h, the expression of CD25 (D), CD69 (E), CD107a (F), TNF-α (G), and IFN-γ (H) on the CAR-T cells was detected by flow cytometry, and the concentrations of TNF-α (I) and IFN-γ (J) in the supernatants was measured using ELISA. All data with error bars represent the mean ± SEM of triplicate values resulting from 3 independent experiments performed under similar conditions. *P<0.05, **P<0.01, ***P<0.001. Student's t-test.

Figure 3. Overexpression of GITRL promotes the proliferation of CAR-T cells and reduces exhaustion.

(A) Number of Control T, PSMA-BB-Z-GITRL, and PSMA-BB-Z-GITRL cells determined by trypan blue exclusion. On day 1, Control T, PSMA-BB-Z and PSMA-BB-Z-GITRL CAR-T cells were co-incubated with PSMA$^+$ PC3 cells at a 1:1 ratio. (B) CAR-T cells were co-cultured with PSMA$^+$ PC3 cells in a 1:1 ratio for 3 days, the relative mRNA expression of *Cdks*, *Aurkb*, and *Mapks* were measured by real-time qPCR. (C and D) After co-culturing CAR-T cells and PSMA$^+$ PC3 cells in a 1:1 ratio for 3 days, the cell cycle and apoptosis of PSMA-BB-Z and PSMA-BB-Z-GITRL CAR-T cells were determined by flow cytometry. (E, F, and G) CAR-T cells were co-cultured with PSMA$^+$ PC3 cells at a 1:1 ratio for 5 days. The proportions of Treg (E), exhaustion molecules PD-1 (F), TIM-3 (F), and the T_{CM} (G) subpopulation in PSMA-BB-Z and PSMA-BB-Z-GITRL CAR-T cells were determined by flow cytometry. All data with error bars represent the mean ± SEM of triplicate values resulting from 3 independent experiments performed under similar conditions. *P<0.05, **P<0.01, ***P<0.001. Student's t-test.

Figure 4. PSMA-BB-Z-GITRL CAR-T cells exhibit stronger proliferation- and NF-κB-related signaling.

(A and B) The MSigDB enrichment bar graph and representative heatmap of differentially expressed genes between PSMA-BB-Z and PSMA-BB-Z-GITRL were generated using the R

663 package pheatmap. (C) GSEA was used to compare the expression profiles of PSMA-BB-Z-GITRL
664 and PSMA-BB-Z based on the HALLMARK_ HALLMARK_MYC TARGETS V1 gene set. (D) GSEA
665 was used to compare the expression profiles of PSMA-BB-Z-GITRL and PSMA-BB-Z based on the
666 HALLMARK_HALLMARK MYC TARGETS V2 gene set. (E) GSEA was used to compare the
667 expression profiles of PSMA-BB-Z-GITRL and PSMA-BB-Z based on the HALLMARK_G2M
668 CHECKPOINT gene set. (F) GSEA was used to compare the expression profiles of PSMA-BB-Z-
669 GITRL and PSMA-BB-Z based on the HALLMARK_P13K AKT MTOR SIGNALING gene set. (G)
670 GSEA was used to compare the expression profiles of PSMA-BB-Z-GITRL and PSMA-BB-Z based
671 on the HALLMARK_E2F TRANSCRIPTION FACTORS gene set. (H) GSEA was used to compare
672 the expression profiles of PSMA-BB-Z-GITRL and PSMA-BB-Z based on the
673 HALLMARK_MTORC1 COMPLEX gene set.
674
675 **Figure 5. GITRL-GITR-mediates the differentiation of PSMA-BB-Z-GITRL CAR-T cells**
676 **towards Th9 and enhancement of their cytotoxicity via the TRAF6-NF-κB pathway.**
677 (A) After co-culturing CAR-T cells with PSMA$^+$ PC3 cells at a 1:1 ratio for 24 hours, the
678 concentration of IL-9 in the co-culture supernatant was measured by ELISA. (B) After co-culturing
679 of CAR-T cells with PSMA$^+$ PC3 cells at a 1:1 ratio for 3 days, the proportion of Th9 cells was
680 detected by flow cytometry. (C) After co-culturing CAR-T cells with PSMA$^+$ PC3 cells at a 1:1 ratio
681 for 24 hours, the fold changes in the expression levels of *Gata3*, *Pu.1*, *Irf4*, and *Traf2*, *Traf5*, and
682 *Traf6* genes in CAR-T cells were measured by qPCR. (D) Western blot analysis of p-P65 and
683 P65 protein level in PSMA-BB-Z and PSMA-BB-Z-GITRL CAR T cells. (E) The CAR-T cells were
684 treated with either vehicle or 10 μM BAY 11-7082 for 30 minutes and then co-cultured with PSMA$^+$
685 PC3 cells at a 1:1 ratio for 24 hours. The concentration of IL-9 in the supernatant was measured
686 by ELISA. (F) CAR-T cells were treated with either vehicle or 10 μM BAY 11-7082 for 30 minutes.
687 The percentage of specific lysis of the CAR-T cells against PSMA$^+$ PC3 cells was determined by
688 luciferase assay at 16 hours of culture, at the indicated E:T ratios. All data with error bars represent
689 the mean ± SEM of triplicate values resulting from 3 independent experiments performed under

similar conditions. ^{NS}P>0.05; **P<0.01; ***P<0.001. Student's t-test.

Figure 6. GITRL reinforces the Anti-tumor Activity of CAR-T cells in mouse model.

(A) Schematic diagram of subcutaneous transplantation and treatment procedure for mouse prostate cancer xenografts. (B and C) Tumor burden measured by bioluminescence at indicated days since Control T, PSMA-BB-Z and PSMA-BB-Z-GITRL CAR-T cells infusion (n=6). (D) Tumor growth curves of individual mice and mean ± s.e.m. values of tumor volume (n=6). (E) Overall survival of mice presented in Kaplan-Meier curves (n=6). (F) The absolute infiltration of $CD3^+CAR^+$ T cells in the blood collected from treated mice was measured on days 7, 14, and 21 (n=6). Data are shown as the mean ± SEM. ***p < 0.001.

Figure 7. PSMA-BB-Z-GITRL CAR T cells exhibited enhanced the systemic anti-tumor activity and persistence in pre-established xenograft solid tumor models.

(A) Schematic diagram of subcutaneous transplantation and treatment procedure for mouse prostate cancer xenografts. (B)The concentrations of IL-9, TNF-α, and IFN-γ in mouse serum were determined by ELISA on day 15 post-treatment (n=5). (C) The proportions of Treg ($CD4^+FOXP3^+$) and T_{CM} cell populations were measured in the peripheral blood of mouse on day 15 post-treatment (n=5). (D) $CD3^+$ T cells absolute infiltration in the spleen collected from treated mouse on day 15 (n=5). (E) Serial sections of tumor tissues treated with PSMA-BB-Z or PSMA-BB-Z-GITRL CAR-T cells were assessed by immunohistochemistry with antibodies for CD3 signals (day 15, n=3). (F) Pathological examination of mouse lungs, livers, kidneys, and hearts was performed using hematoxylin and eosin (HE) staining on day 15 of treatment. (G) Experimental schematic of PC3-PSMA-LUC tumor re-challenge with PSMA-BB-Z-GITRL CAR-T cells. PSMA-BB-Z-GITRL CAR T cells-treated mouse that showed no detectable tumor were subcutaneous transplantation implanted with 2 million PC3-PSMA-LUC cells on day 28. As control, naïve mice were implanted with PC3-PSMA-LUC cells following an injection of Control T cells. (H) Tumor burden measured by bioluminescence at indicated days since PSMA-BB-Z-GITRL CAR-T cell infusion (n=5). Data are

717 shown as the mean ± SEM. *p < 0.05, **p < 0.01, ***p < 0.001.

Journal Pre-proof

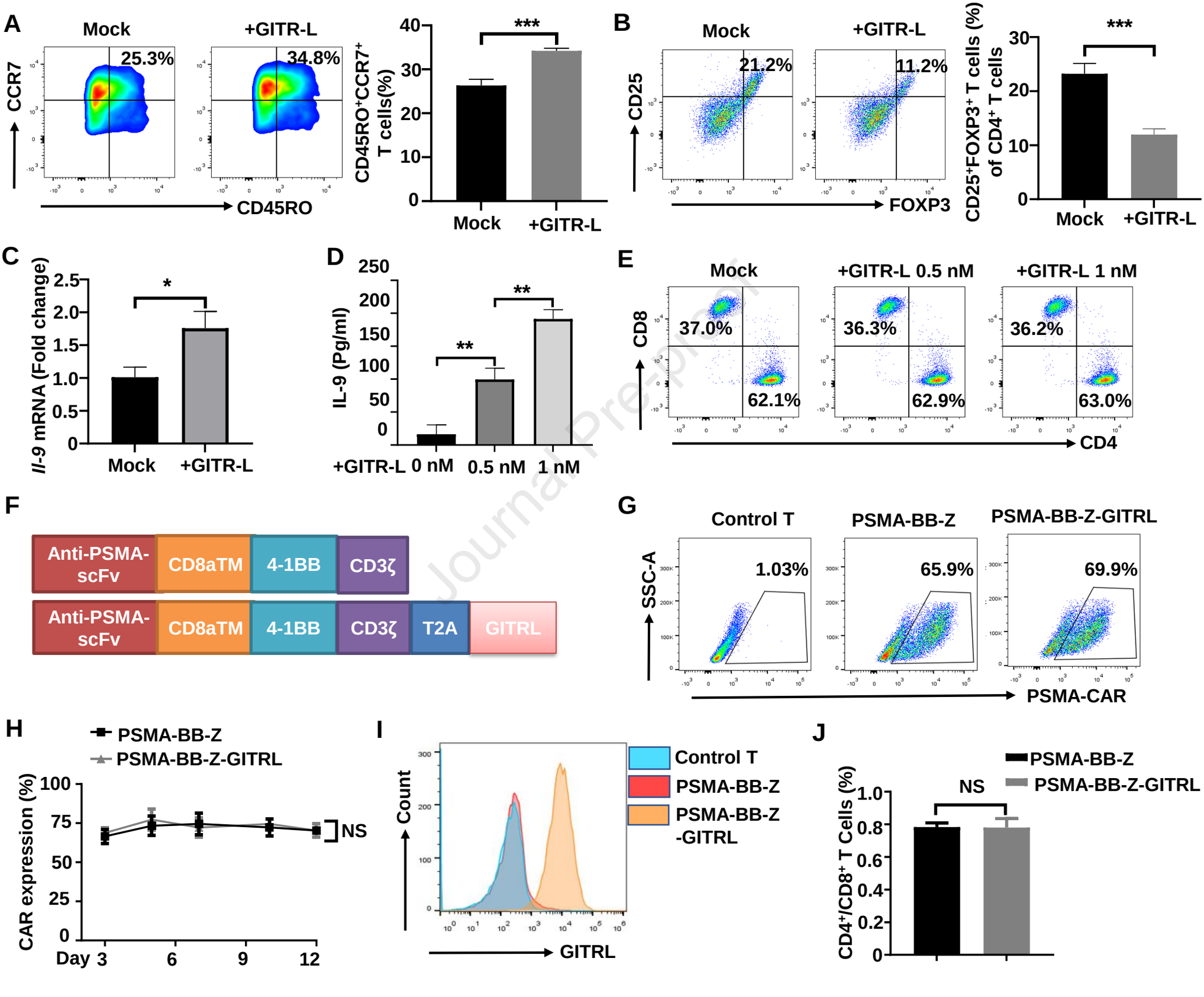
A
Mock
+GITR-L
25.3%
34.8%
CCR7
CD45RO
CD45RO+CCR7+ T cells(%)
***
Mock
+GITR-L
B
Mock
+GITR-L
21.2%
11.2%
CD25
FOXP3
CD25+FOXP3+ T cells (%) of CD4+ T cells
***
Mock
+GITR-L
C
Il-9 mRNA (Fold change)
*
Mock
+GITR-L
D
IL-9 (Pg/ml)
**
**
+GITR-L 0 nM
0.5 nM
1 nM
E
Mock
+GITR-L 0.5 nM
+GITR-L 1 nM
37.0%
62.1%
36.3%
62.9%
36.2%
63.0%
CD8
CD4
F
Anti-PSMA-scFv
CD8aTM
4-1BB
CD3ζ
Anti-PSMA-scFv
CD8aTM
4-1BB
CD3ζ
T2A
GITRL
G
Control T
PSMA-BB-Z
PSMA-BB-Z-GITRL
1.03%
65.9%
69.9%
SSC-A
PSMA-CAR
H
PSMA-BB-Z
PSMA-BB-Z-GITRL
CAR expression (%)
NS
Day 3
6
9
12
I
Count
Control T
PSMA-BB-Z
PSMA-BB-Z -GITRL
GITRL
J
PSMA-BB-Z
PSMA-BB-Z-GITRL
NS
CD4+/CD8+ T Cells (%)

Journal Pre-proof

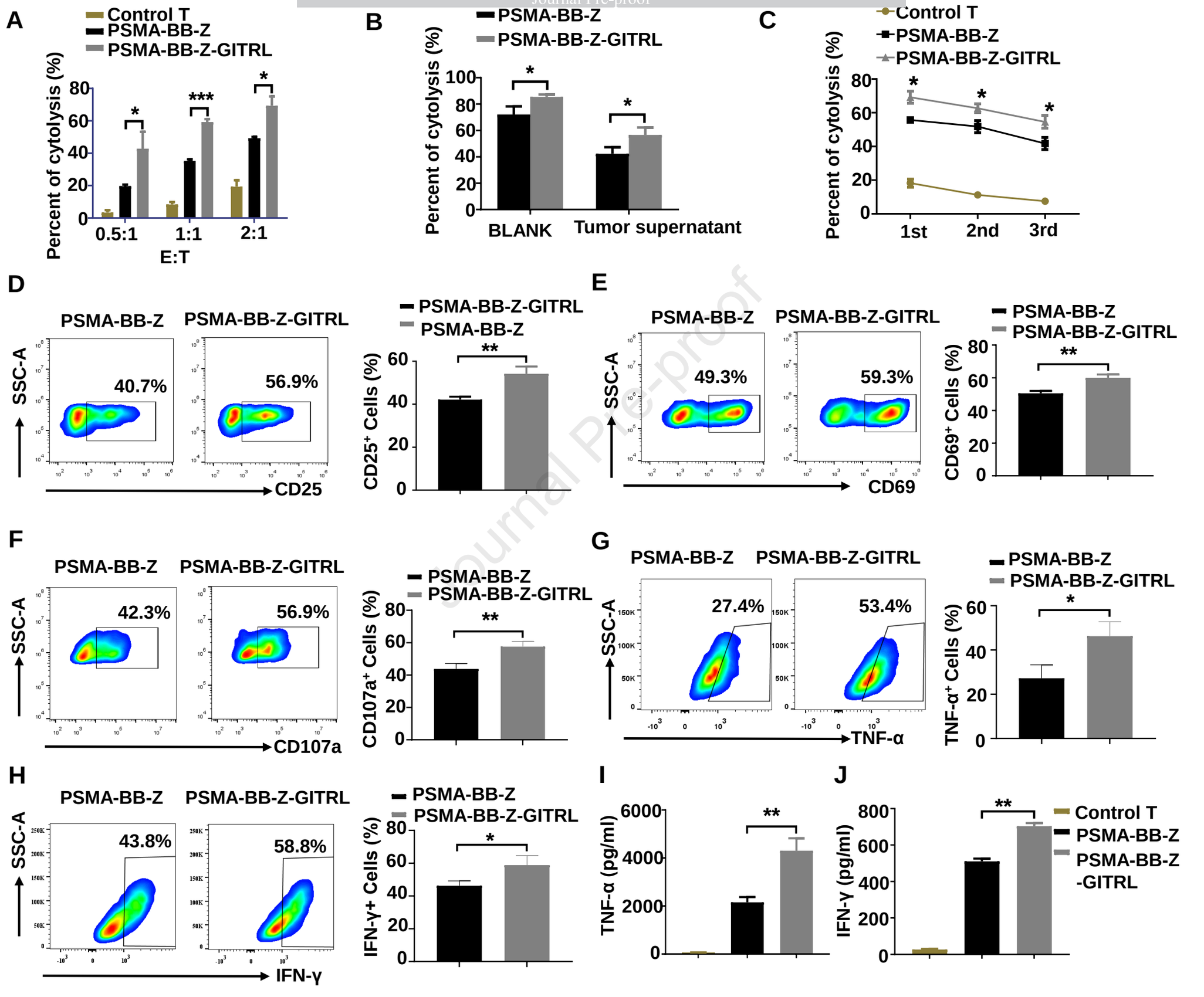

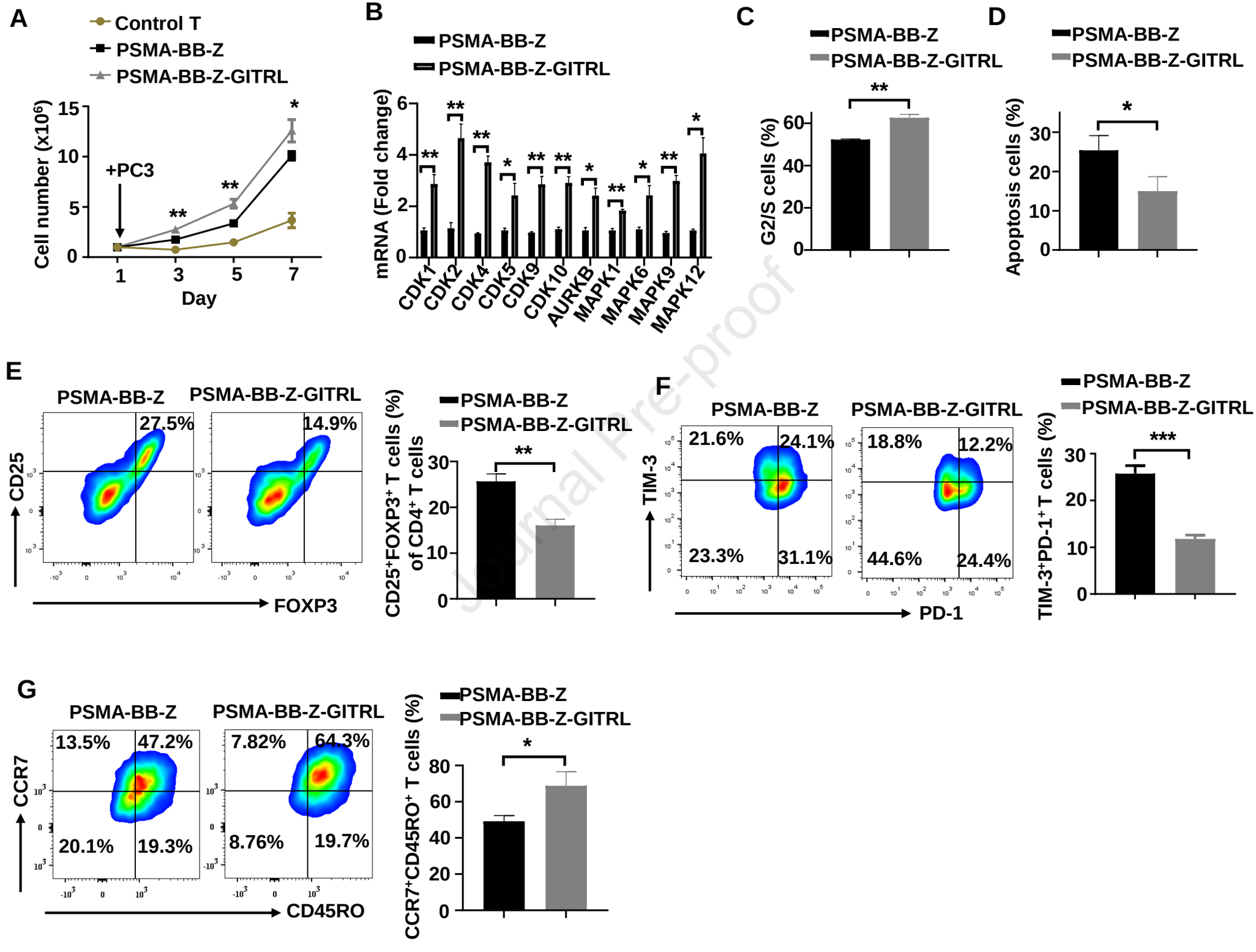
A
Control T
PSMA-BB-Z
PSMA-BB-Z-GITRL
Cell number (x10^6)
+PC3
Day
B
PSMA-BB-Z
PSMA-BB-Z-GITRL
mRNA (Fold change)
CDK1
CDK2
CDK4
CDK5
CDK9
CDK10
AURKB
MAPK1
MAPK6
MAPK9
MAPK12
C
PSMA-BB-Z
PSMA-BB-Z-GITRL
G2/S cells (%)
D
PSMA-BB-Z
PSMA-BB-Z-GITRL
Apoptosis cells (%)
E
PSMA-BB-Z
PSMA-BB-Z-GITRL
27.5%
14.9%
CD25
FOXP3
CD25+FOXP3+ T cells (%) of CD4+ T cells
PSMA-BB-Z
PSMA-BB-Z-GITRL
F
PSMA-BB-Z
PSMA-BB-Z-GITRL
21.6%
24.1%
23.3%
31.1%
18.8%
12.2%
44.6%
24.4%
TIM-3
PD-1
TIM-3+PD-1+ T cells (%)
PSMA-BB-Z
PSMA-BB-Z-GITRL
G
PSMA-BB-Z
PSMA-BB-Z-GITRL
13.5%
47.2%
20.1%
19.3%
7.82%
64.3%
8.76%
19.7%
CCR7
CD45RO
CCR7+CD45RO+ T cells (%)
PSMA-BB-Z
PSMA-BB-Z-GITRL

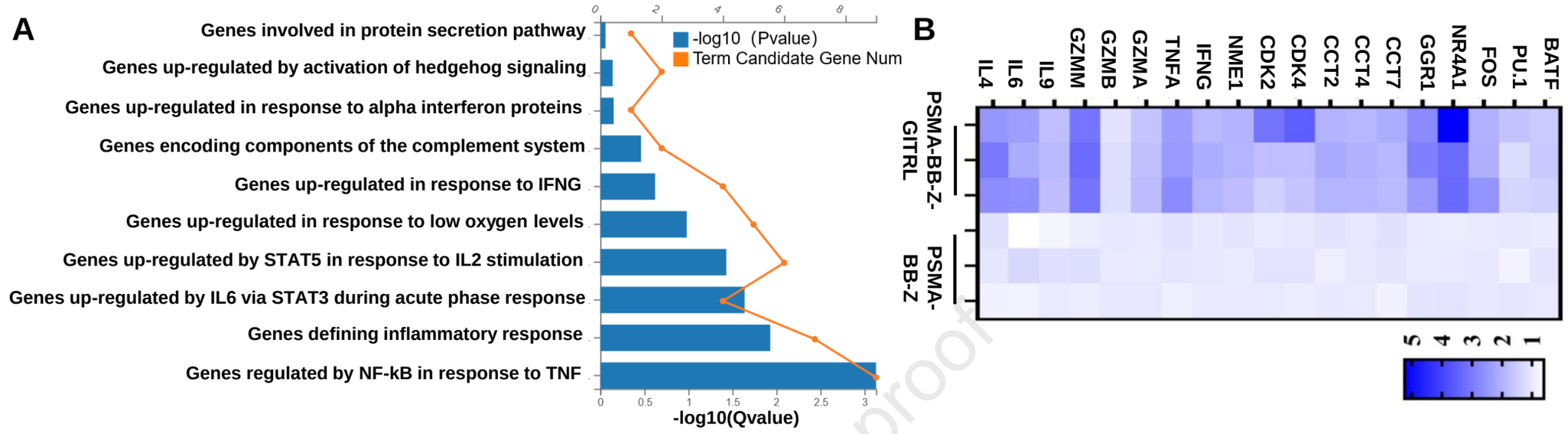
A
Genes involved in protein secretion pathway
Genes up-regulated by activation of hedgehog signaling
Genes up-regulated in response to alpha interferon proteins
Genes encoding components of the complement system
Genes up-regulated in response to IFNG
Genes up-regulated in response to low oxygen levels
Genes up-regulated by STAT5 in response to IL2 stimulation
Genes up-regulated by IL6 via STAT3 during acute phase response
Genes defining inflammatory response
Genes regulated by NF-kB in response to TNF
-log10 (Pvalue)
Term Candidate Gene Num
-log10(Qvalue)
B
IL4
IL6
IL9
GZMM
GZMB
GZMA
TNFA
IFNG
NME1
CDK2
CDK4
CCT2
CCT4
CCT7
GGR1
NR4A1
FOS
PU.1
BATF
PSMA-BB-Z-GITRL
PSMA-BB-Z

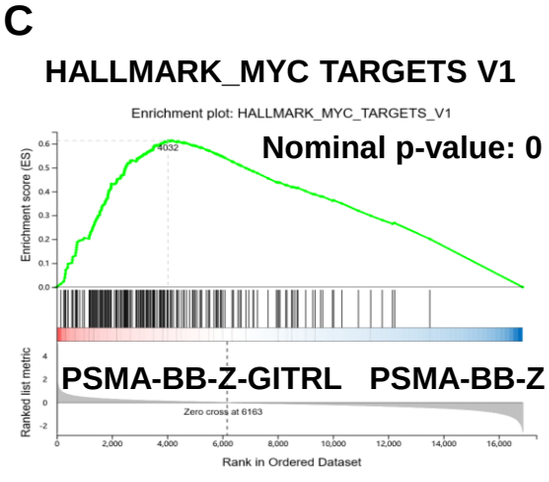
C
HALLMARK_MYC TARGETS V1
Enrichment plot: HALLMARK_MYC_TARGETS_V1
Nominal p-value: 0
Signal2Noise
Enrichment Profile
Hits
Ranking metric scor
Enrichment score (ES)
Ranked list metric
PSMA-BB-Z-GITRL
PSMA-BB-Z
Zero cross at 6163
Rank in Ordered Dataset

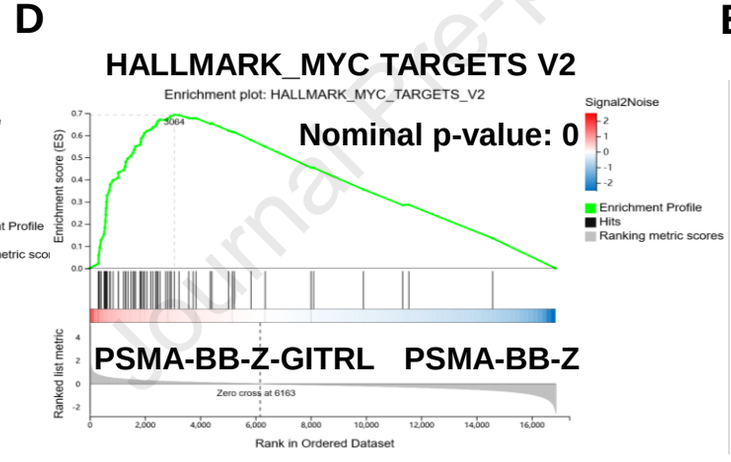
D
HALLMARK_MYC TARGETS V2
Enrichment plot: HALLMARK_MYC_TARGETS_V2
Nominal p-value: 0
Signal2Noise
Enrichment Profile
Hits
Ranking metric scores
Enrichment score (ES)
Ranked list metric
PSMA-BB-Z-GITRL
PSMA-BB-Z
Zero cross at 6163
Rank in Ordered Dataset

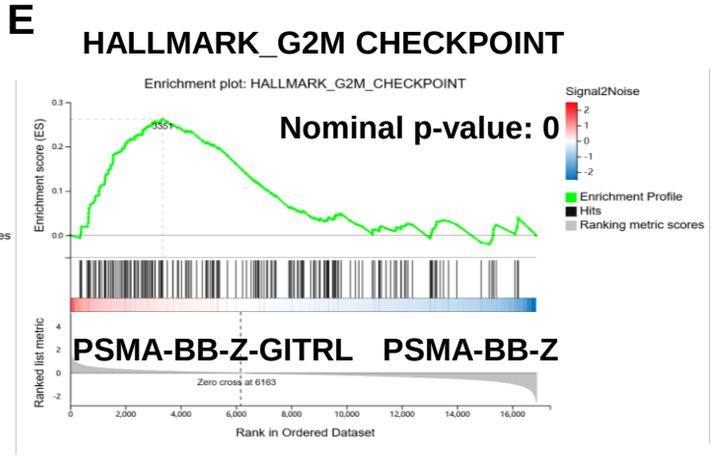
E
HALLMARK_G2M CHECKPOINT
Enrichment plot: HALLMARK_G2M_CHECKPOINT
Nominal p-value: 0
Signal2Noise
Enrichment Profile
Hits
Ranking metric scores
Enrichment score (ES)
Ranked list metric
PSMA-BB-Z-GITRL
PSMA-BB-Z
Zero cross at 6163
Rank in Ordered Dataset

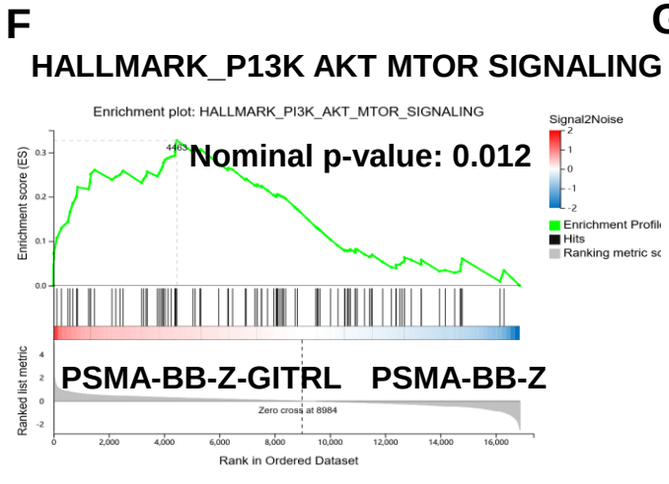
F
HALLMARK_P13K AKT MTOR SIGNALING
Enrichment plot: HALLMARK_PI3K_AKT_MTOR_SIGNALING
Nominal p-value: 0.012
Signal2Noise
Enrichment Profil
Hits
Ranking metric sc
Enrichment score (ES)
Ranked list metric
PSMA-BB-Z-GITRL
PSMA-BB-Z
Zero cross at 8984
Rank in Ordered Dataset

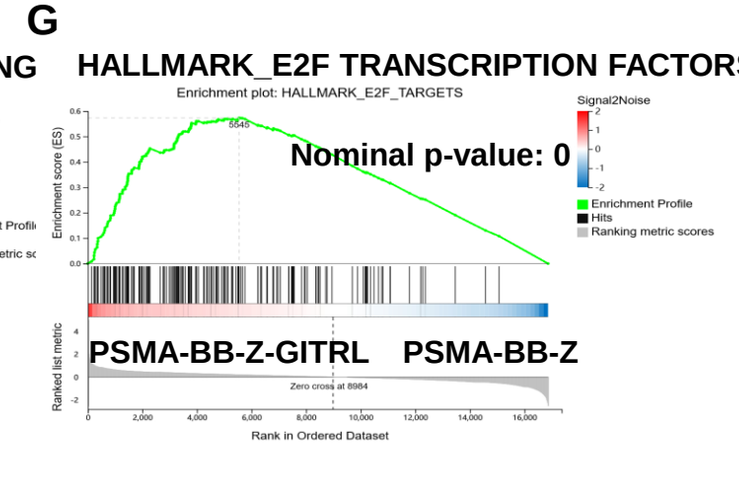
G
HALLMARK_E2F TRANSCRIPTION FACTORS
Enrichment plot: HALLMARK_E2F_TARGETS
Nominal p-value: 0
Signal2Noise
Enrichment Profile
Hits
Ranking metric scores
Enrichment score (ES)
Ranked list metric
PSMA-BB-Z-GITRL
PSMA-BB-Z
Zero cross at 8984
Rank in Ordered Dataset

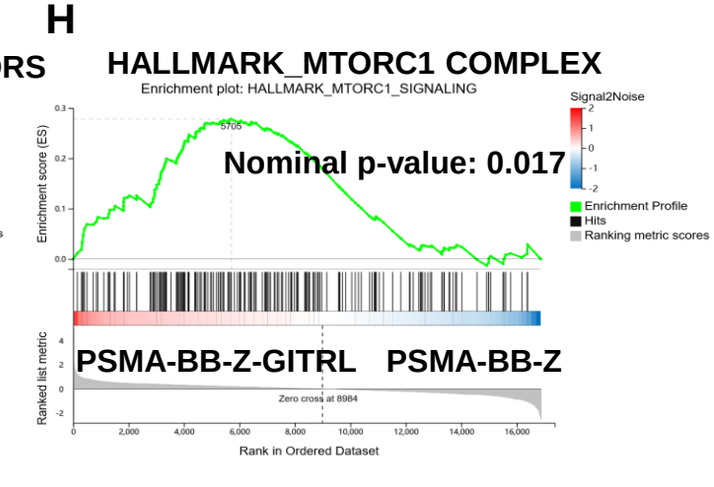
H
HALLMARK_MTORC1 COMPLEX
Enrichment plot: HALLMARK_MTORC1_SIGNALING
Nominal p-value: 0.017
Signal2Noise
Enrichment Profile
Hits
Ranking metric scores
Enrichment score (ES)
Ranked list metric
PSMA-BB-Z-GITRL
PSMA-BB-Z
Zero cross at 8984
Rank in Ordered Dataset

Journal Pre-proof

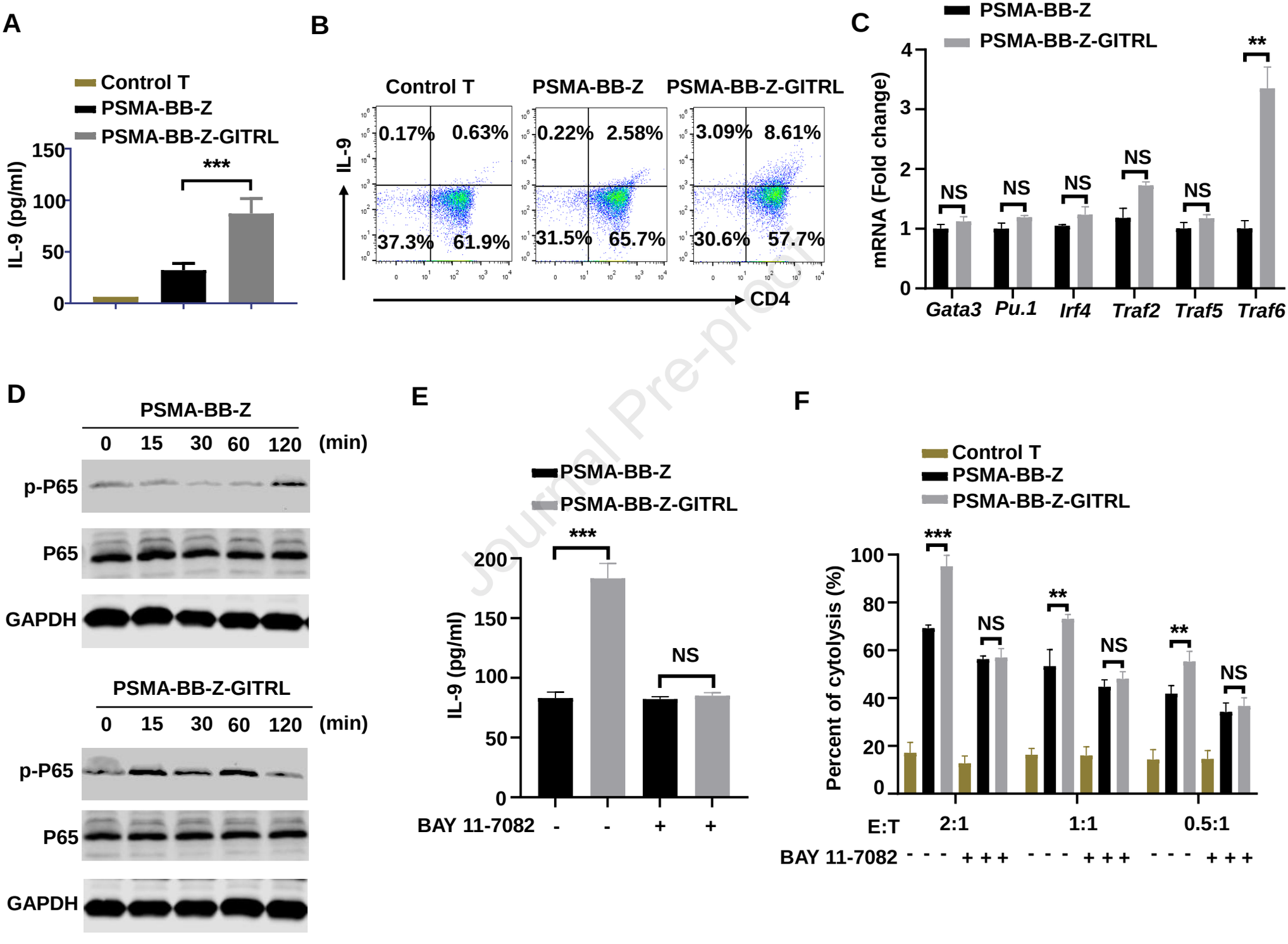

Journal Pre-proof

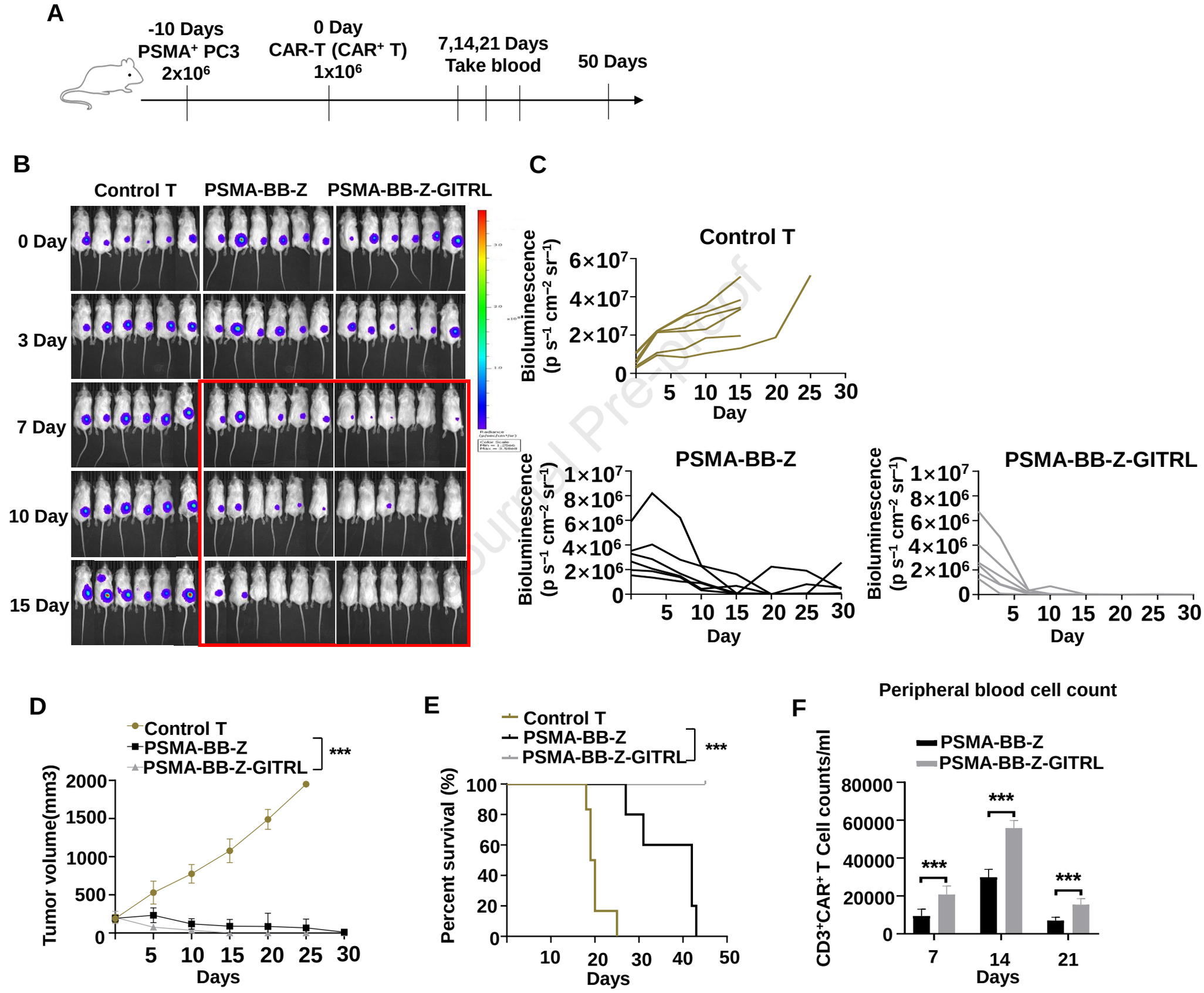

Journal Pre-proof

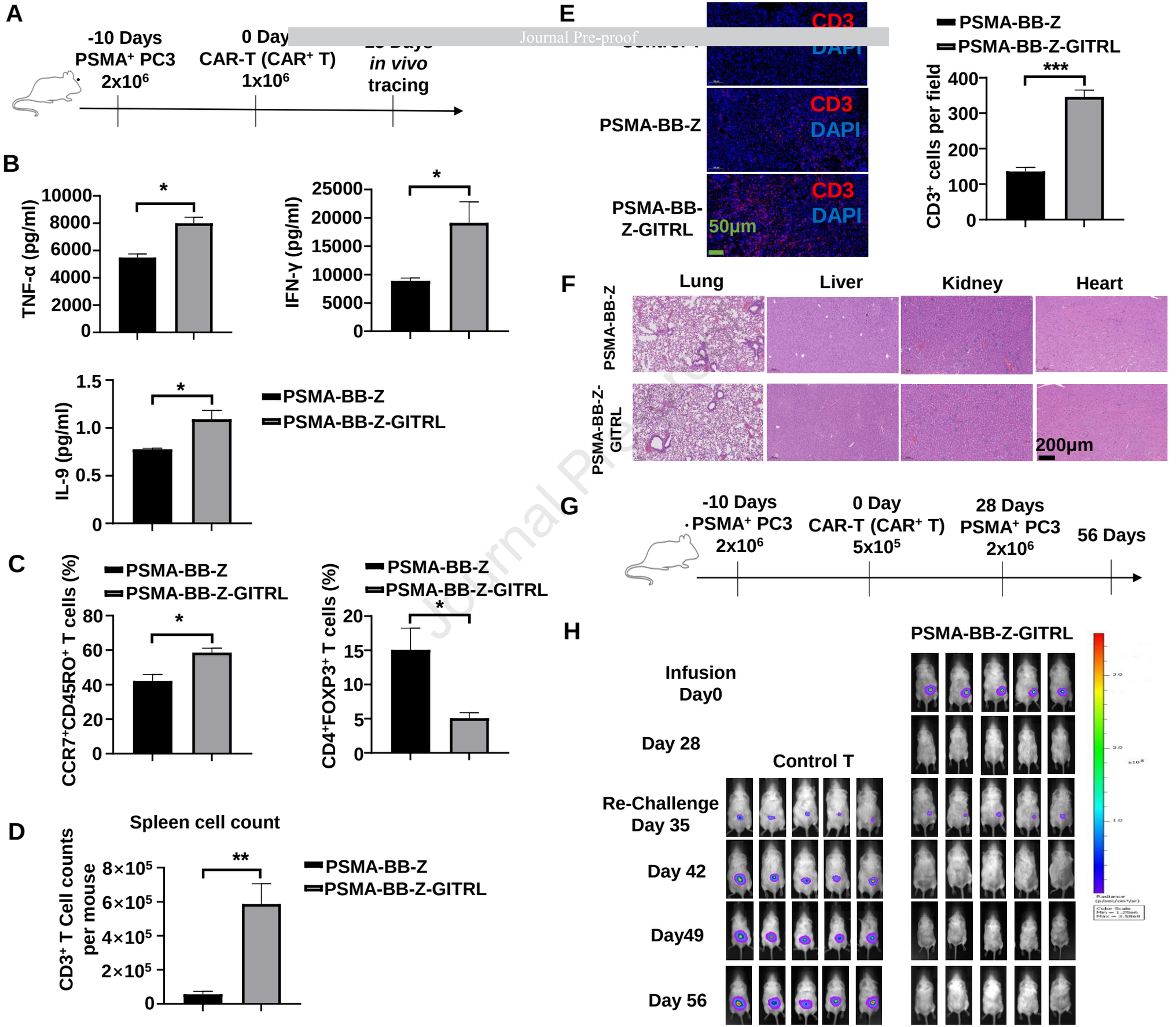

Du and colleagues established a novel enhanced CAR-T cells co-expressing GITRL that could activate the GITR-TRAF6-NF-κB pathway and promote CAR-T cells proliferation and differentiation toward Th9 and T_{CM}, thereby enhanced cytotoxicity against solid tumors.

Journal Pre-proof